Biomedicine & Pharmacotherapy 165 (2023) 115153

Contents lists available at ScienceDirect

Biomedicine & Pharmacotherapy

journal homepage: www.elsevier.com/locate/biopha

Sodium Danshensu stabilizes atherosclerotic vulnerable plaques by targeting IKKβ mediated inflammation in macrophages

Miao Zeng [a,1], Xiaolu Zhang [a,1], Nuan Lv [a], Luming Wang [a], Yanrong Suo [b], Jiali Gan [a], Lin Yang [a], Bin Yu [a], Xijuan Jiang [a,*], Wenyun Zeng [c,*]

[a] School of Integrative Medicine, Tianjin University of Traditional Chinese Medicine, Tianjin 301617, China
[b] Traditional Chinese Medicine Department, Ganzhou People's Hospital, Ganzhou 341000, China
[c] Oncology Department, Ganzhou People's Hospital, Ganzhou 341000, China

ARTICLE INFO

Keywords:
Atherosclerosis
Sodium Danshensu
IKKβ
Inflammation
Macrophage

ABSTRACT

Background: The primary cause of acute cardiovascular events with high mortality is the rupture of atherosclerotic plaque followed by thrombosis. Sodium Danshensu (SDSS) has shown potential in inhibiting the inflammatory response in macrophages and preventing early plaque formation in atherosclerotic mice. However, the specific targets and detailed mechanism of action of SDSS are still unclear.

Objective: This study aims to investigate the efficacy and mechanism of SDSS in inhibiting inflammation in macrophages and stabilizing vulnerable plaques in atherosclerosis (AS).

Materials and Methods: The efficacy of SDSS in stabilizing vulnerable plaques was demonstrated using various techniques such as ultrasound, Oil Red O staining, HE staining, Masson staining, immunohistochemistry, and lipid analysis in ApoE$^{-/-}$ mice. Subsequently, IKKβ was identified as a potential target of SDSS through protein microarray, network pharmacology analysis, and molecular docking. Additionally, ELISA, RT-qPCR, Western blotting, and immunofluorescence were employed to measure the levels of inflammatory cytokines, IKKβ, and NF-κB pathway-related targets, thereby confirming the mechanism of SDSS in treating AS both in vivo and in vitro. Finally, the impact of SDSS was observed in the presence of an IKKβ-specific inhibitor.

Results: Initially, the administration of SDSS led to a decrease in the formation and area of aortic plaque, while also stabilizing vulnerable plaques in ApoE$^{-/-}$ mice. Furthermore, it was identified that IKKβ serves as the primary binding target of SDSS. Additionally, both in vivo and in vitro experiments demonstrated that SDSS effectively inhibits the NF-κB pathway by targeting IKKβ. Lastly, the combined use of the IKKβ-specific inhibitor IMD-0354 further enhanced the beneficial effects of SDSS.

Conclusions: SDSS stabilized vulnerable plaques and suppressed inflammatory responses by inhibiting the NF-κB pathway through its targeting of IKKβ.

1. Introduction

Atherosclerosis (AS) is a chronic inflammatory disease driven by lipids, which can lead to life-threatening complications such as acute myocardial infarction, stroke, and aortic aneurysm [1]. Within atherosclerotic plaques, there are two types: vulnerable plaques, which have a high risk of rupture, and stable plaques, which have a lower risk of rupture [2–5]. Vulnerable plaques are typically characterized by thin

Abbreviations: AS, Atherosclerosis; ApoE$^{-/-}$, Apolipoprotein E-deficient; BP, Biological process; CCK-8, Cell Counting Kit-8 assay; CC, Cellular component; DAB, Diaminobenzidine; GO, Gene Ontology; HDL-C, High-density lipoprotein cholesterol; HE, Hematoxylin-eosin; IL-1R, Interleukin-1 receptor; IKK, IκB kinase; KEGG, Kyoto Encyclopedia of Genes and Genomes; LDL-C, Low-density lipoprotein cholesterol; LDH, Lactate dehydrogenase; MOMA-2, Monocyte/macrophage antigen-2; MF, Molecular function; NF-κB, Nuclear factor-κB; Ox-LDL, Oxidized low-density lipoprotein; OCT, Optimum cutting temperature; PPI, protein-protein interaction; PVDF, Polyvinylidene fluoride; PEG, Polyethylene glycol; SDSS, Sodium Danshensu; SPF, Specific pathogen-free; SNR, Signal-to-noise ratio; SDS-PAGE, Sodium dodecyl sulfate polyacrylamide gel electrophoresis; SD, standard deviation; SMC, Smooth muscle cells; TC, Total cholesterol; TG, Triglyceride; TNFR, Tumor necrosis factor receptor; TLR, Toll-like receptor; α-SMA, α-smooth muscle actin.

* Corresponding authors.
E-mail addresses: jxj2668@tjutcm.edu.cn (X. Jiang), zengwenyun@foxmail.com (W. Zeng).
[1] These authors have contributed equally to this work.

https://doi.org/10.1016/j.biopha.2023.115153
Received 21 May 2023; Received in revised form 2 July 2023; Accepted 7 July 2023
Available online 10 July 2023

fibrous caps, high lipid content, increased lymphocytes, and increased apoptotic macrophages [6]. In some cases, the stenosis caused by vulnerable plaques may not be very severe, but the risk of rupture, bleeding, thrombosis, or spasm is higher compared to stable plaques. If the vulnerable plaque can be transformed into a more stable plaque, it will have a beneficial impact on the clinical prevention of acute cardiovascular or cerebrovascular diseases [7].

Previous studies have confirmed a high level of macrophage infiltration in the vulnerable plaque of patients with AS, with significantly more macrophages compared to stable plaques [8]. Inhibiting macrophage proliferation and infiltration in vulnerable AS plaques has the potential to reduce the inflammatory response [9], thus preventing plaque rupture. Additionally, the activation of the canonical nuclear factor-κB (NF-κB) signaling pathway mediated by IKKβ, plays a crucial role in regulating inflammatory processes and is closely associated with the onset and progression of AS [10]. In studies conducted on both human and animal models of AS, it has been observed that the NF-κB signaling pathway is activated in macrophages, endothelial cells, and smooth muscle cells present in plaques [11]. Previous research has demonstrated that NF-κB activation in AS patients relies on IKKβ, which results in the up-regulation of pro-inflammatory cytokines and prothrombotic mediators. Meanwhile, the phosphorylation of IKKβ, IκB, and p65 is induced by oxidized low-density lipoprotein (ox-LDL) in THP-1 macrophages [12]. Moreover, inhibiting the expression of IKKβ significantly reduces the phosphorylation level of NF-κB in ox-LDL-stimulated macrophages [13]. Myeloid-specific IKKβ deficiency was found to suppress inflammatory responses in macrophages, including adhesion, migration, and lipid uptake. This ultimately led to a reduction in the size of high-fat-induced plaques in $LDLR^{-/-}$ mice [14]. Therefore, the activation of the NF-κB signaling pathway, mediated by IKKβ in macrophages, plays a crucial role in promoting the progression of AS.

Danshensu, a water-soluble phenolic acid component found in Danshen (*Salvia miltiorrhiza Bunge*) [15], prevents atherosclerosis through three main mechanisms: endothelial protection, macrophage regulation, and lipidemia control [16]. Danlou tablets (containing Danshensu as one of the main ingredients) attenuated the plaque size and reduced lipid content in the brachiocephalic trunk, aortic arch, and aortic root of apolipoprotein E-deficient ($ApoE^{-/-}$) mice fed a high-fat diet for 20 weeks [17]. In addition, Danshensu has demonstrated its ability to prevent AS by inhibiting the TLR4/NF-κB signaling pathway in a high-fat diet-induced AS rat model [18]. Danshensu directly inhibits the secretion of TNF, IL-1, IL-6, and IL-8, and suppresses the inflammatory activation of macrophages [19]. Sodium Danshensu [SDSS, sodium D-(+)-β-(3,4-dihydroxyphenyl) lactate, $C_9H_9O_5Na$, Fig. 3A], the stable form of Danshensu, has the same medicinal properties [20]. However, the potential of SDSS to stabilize vulnerable plaques in AS and its underlying mechanism are still unknown. Therefore, in this study, male $ApoE^{-/-}$ mice were fed a high-fat diet for 24 weeks to establish the vulnerable plaque model, and J774A.1 monocyte-macrophages were treated with ox-LDL to replicate the cell inflammation model. Following the administration of SDSS, it was shown that SDSS can effectively stabilize vulnerable AS plaques in $ApoE^{-/-}$ mice and reduce macrophage-mediated inflammatory responses by targeting the upstream kinase IKKβ in the NF-κB signaling pathway.

2. Materials and methods

2.1. Regents

SDSS was purchased from Shanghai Yuanye Biotechnology Co., Ltd. (Shanghai, China). Atorvastatin was purchased from Sigma-Aldrich (MO, USA).

2.2. Animal husbandry and drug administration

Specific pathogen-free (SPF) grade male $ApoE^{-/-}$ mice and C57BL/6 J mice were obtained from Beijing Weitong Lihua Experimental Animal Technology Co., Ltd. [Certificate No.: SCXK (JING) 2016–0006] at the age of 7–8 weeks and weighing 18–20 g. The mice were housed in a controlled environment (temperature 22 ± 2 ℃, humidity 50 ± 10%) with a 12 h light/dark cycle. They had ad libitum access to food and water. All animal handling procedures were performed in accordance with the guidelines of the Experimental Animal Ethics Committee of Tianjin University of Traditional Chinese Medicine (Animal Experiment Ethics No.: TCM-LAEC2020110).

One week after acclimatization, C57BL/6 J mice were fed with normal diet as a control group (Control). $ApoE^{-/-}$ mice that were fed high-fat diet (0.15% cholesterol + 21% fat) were randomly divided into model group (Model), SDSS low-dose treatment group (SDSS40, 40 mg/kg/d), SDSS high-dose treatment group (SDSS80, 80 mg/kg/d), and atorvastatin treatment group (Atorvastatin, 10 mg/kg/d). After 12 weeks of feeding, the mice in the control and model groups were injected intraperitoneally with normal saline for 12 weeks, and at the same time control group was given normal diet and the model group was given high-fat diet. Meanwhile, mice in the SDSS low-dose, SDSS high-dose, and atorvastatin groups were injected intraperitoneally with SDSS (40 mg/kg/d, 80 mg/kg/d), and atorvastatin (10 mg/kg/d) respectively, for 12 weeks while continuing to be fed a high-fat diet.

2.3. High frequency ultrasound technology and lipid analysis

Mice were anesthetized by ether inhalation, and plaques in the aortic arch were assessed using High Frequency Ultrasound Imaging System (Vevo 2100, USA) with a 40 MHz transducer. Serum levels of total cholesterol (TC), triglyceride (TG), low-density lipoprotein cholesterol (LDL-C), and high-density lipoprotein cholesterol (HDL-C) were measured using commercially available kits (Nanjing Jiancheng Bioengineering Institute, Nanjing, China).

2.4. Oil Red O, Hematoxylin-eosin and masson staining

The entire aortas (from the aortic arch to the iliac bifurcation with brachiocephalic trunk) were isolated and cut longitudinally, then fixed in 4% paraformaldehyde for 48 h. The fresh aortic root was then frozen in optimum cutting temperature (OCT) compound and sectioned at 8 μm thickness. Furthermore, aortic roots were fixed in 4% paraformaldehyde for 48 h, then embedded in paraffin and sectioned to slices with thickness of 5 μm. *En face* preparations and frozen aortic roots sections were briefly immersed in 60% isopropanol, and stained with 0.6% Oil-Red-O solution for 15–20 min. Paraffin-embedded aortic root sections were stained with hematoxylin-eosin (HE) and Masson staining using standard methods. Images were captured using a light microscope (Leica DM3000, Germany) and a stereoscopic dissecting microscope before analysis using Image J software.

2.5. Immunohistochemistry

Immunohistochemistry was performed on paraffin sections of mouse aortic roots using primary antibodies against monocyte/macrophage antigen-2 (MOMA-2, Abcam, Cambridge, MA) and α-smooth muscle actin (α-SMA, Abcam, Cambridge, MA) to identify macrophages and smooth muscle cells, followed by their corresponding secondary antibodies conjugated to horseradish peroxidase (BOSTER, Wuhan, China). Stains were developed using diaminobenzidine (DAB) and images were captured using a Leica scanning electron microscope and analysed using Image J software.

2.6. Huprot^{TM} human protein microarray

Human protein microarray assay and data analysis were performed by a commercial company Wayen Biotechnologies, Inc. (Shanghai, China), according to a previously published procedure [21]. The protein microarray chip contains 20,000 proteins. Signal-to-noise ratio (SNR) was calculated as the ratio of foreground to background values. For each protein dot, a SDSS-Biotin group signal to a Biotin group signal (IMean_Ratio) $\geq$ 1.4 was considered as positive result, indicating its binding to SDSS.

2.7. Network pharmacology analysis and molecular docking

Targets associated with the disease "atherosclerosis" were collected from the OMIM (https://www. omim.org/), DisGeNET (https://www.disgenet.org), and PharmGKB (https://www.pharmgkb.org) databases and duplicate targets were eliminated. The disease targets identified in the database were intersected with proteins capable of binding to SDSS to identify the targets of SDSS relevant to atherosclerosis. The intersection targets were imported into the STRING database (https://string-db.org), where a protein-protein interaction (PPI) network was constructed. The network was visualized using Cytoscape 3.7.1 software. The topological parameters of PPI network were analyzed using the Network Analyzer plug-in in Cytoscape. The core targets were identified based on a degree greater than or equal to the median. Gene Ontology (GO) functional annotations and Kyoto Encyclopedia of Genes and Genomes (KEGG) pathways of the candidate core targets were enriched using DAVID 6.8 (https://david.ncifcrf.gov). The downloaded results were sorted based on the number of targets and P values. GO enrichment analysis and KEGG pathway analysis were performed using an online data analysis and visualization platform (http://www.bioinformatics.com. cn) respectively.

To begin, the crystal structures of the IKKβ and NFKB1 proteins were acquired from the Protein Data Bank (PDB, PDB codes: 4KIK and 2O61 respectively). These structures need to undergo dehydration and hydrogenation before the docking process. The 3D structure of SDSS was obtained from the PubChem Compound database. Autodock analysis was performed using Autodock 4.2.6 software, employing the semi-flexible docking method. The docking process was carried out with the following parameter settings: Gasteiger charges and polar hydrogen were added to both small molecules and proteins. The grid box size was set to 60 × 60 × 60, and the grid spacing was set to 0.375 Å. Each ligand was docked 100 times using the Lamarckian genetic algorithm, with a total energy evaluation set to 2,500,000. After the docking process, 50 conformations were obtained for clustering analysis, with an RMSD equal to 0.2 nm. The conformations with the lowest energy and the highest number of clusters were selected for the subsequent research step. Finally, the docking results were visualized using PyMOL software.

2.8. Cell culture

The murine macrophage J774A.1 cell line was purchased from Beijing BeiNa Biotechnology Institute. Cells were cultured at 1×10^6 cells/ml in DMEM medium (Gibco, New York, USA) containing 10% FBS and 1% antibiotics (penicillin, 100 IU/ml; streptomycin, 100 μg/ml) and incubated a humidified chamber with 5% CO_2 at 37 ℃. To evaluate the effect of SDSS on ox-LDL-induced macrophage inflammation and IKKβ/NF-κB pathway activation (experiment 1), J774A.1 cells were divided into six groups: control group (Control), model group (Model, ox-LDL), SDSS group (SDSS12.5, SDSS25, SDSS50, SDSS100 groups with 12.5 μM, 25 μM, 50 μM, 100 μM of SDSS administration respectively). Cells in the Model and SDSS groups were treated with ox-LDL (Yiyuan Biotechnology, Guangzhou, China) for 24 h to induce macrophage inflammatory response and then treated with SDSS (12.5 μM, 25 μM, 50 μM, 100 μM) for 24 h before analysis.

What's more, the next experiment intervened with IMD-0354, a specific inhibitor of IKKβ, was used to observe the pharmacodynamic changes of SDSS (experiment 2). J774A.1 cells were divided into five groups: control group (Control), model group (Model, ox-LDL), SDSS group (SDSS50, 50 μM), IMD-0354 group (IMD, 1 μM), SDSS+IMD-0354 group (SDSS50-IMD, 50 μM SDSS+1 μM IMD-0354). Cells in the Model, SDSS50, and SDSS50-IMD groups were treated with ox-LDL for 24 h, then SDSS50 and SDSS50-IMD groups were treated with 50 μM SDSS and 50 μM SDSS+ 1 μM IMD-0354 for 24 h respectively before analysis.

2.9. CCK8, LDH, and ELISA

Following cell death, cytoplasmic lactate dehydrogenase (LDH) was released into the culture medium. The supernatant was then collected in 96-well plates and assessed using a Lactate dehydrogenase assay kit (Jiancheng Bioengineering Institute, Nanjing, China) following the manufacturer's instructions. The absorbance values were measured at 450 nm. Cell viability was assessed using the Cell Counting Kit-8 assay (CCK-8, Dojindo, Kumamoto, Japan). Briefly, cells were seeded at a density of 1×10^5 cells/well in 96-well plates. Then, 10 μl CCK-8 reagent was added to each well. After incubating the cells at 37 ℃ for 1 h, the absorbance was measured at a wavelength of 450 nm using a microplate reader. Cell culture supernatant and serum were assayed using ELISA kits for TNF-α (MultiSciences Biotech, Hangzhou, China), IL-1β (MultiSciences Biotech, Hangzhou, China), and IL-6 (Wuhan ColorfulGene Biological Technology Co., Ltd., Wuhan, China).

2.10. Quantitative RT-qPCR analysis

Total RNA and protein were extracted from mouse aorta and J774A.1 cells using the DNA/RNA/Protein Isolation Kit. Subsequently, the total RNA was reverse transcribed into cDNA using a reverse transcription kit. The RT-qPCR procedures were as follows: pre-denaturation at 95 ℃ for 10 min, denaturation at 95 ℃ for 15 s, annealing and elongation at 60 ℃ for 1 min, 40 cycles. The relative amount of mRNA was determined using the $2^{-\Delta\Delta CT}$ method. The primers for RT-qPCR were synthesized by Sangon Biotech (Shanghai) Co., Ltd and are listed in Table S1.

2.11. Western blotting analysis

Total protein was extracted from mouse aorta and J774A.1 cells then quantified using the BCA protein assay. The protein extracts were denatured, then separated using sodium dodecyl sulfate polyacrylamide gel electrophoresis (SDS-PAGE) electrophoresis. After that, the separated proteins were transferred to a Polyvinylidene fluoride (PVDF) membrane, and blocked with 5% skim milk to prevent non-specific bindings. Primary antibodies against IKKβ (1:1000, 2370 S, Cell Signaling Technology, USA), p-IKKβ (1:500, 2697 T, Cell Signaling Technology, USA), IκBα (1:1000, 4812 S, Cell Signaling Technology, USA), p-IκBα (1:500, 9246 S, Cell Signaling Technology, USA), NF-κB (p65, 8242 S, 1:1000, Cell Signaling Technology, USA), p-p65 (1:500, 3033 S, Cell Signaling Technology, USA), TNF-α (1:500, AF7014, Affinity Biosciences, USA), IL-1β (1:500, ab9722, Abcam, Cambridge, MA), TLR4 (1:500, sc-293072, Santa Cruz, Dallas, USA), or GAPDH (1:10000, ab181602, Abcam, Cambridge, MA) were applied to incubate overnight at 4 ℃. Secondary antibody (1:10000, 7074 S, 7076 S, Cell Signaling Technology, USA) was applied to incubate for 2 h and visualized by chemiluminescence. The ratio of the gray value of the target protein band to that of GAPDH band in the same sample indicated the relative expression of the target protein.

2.12. Immunofluorescence

Sections of frozen aorta root was permeabilized with 0.3% Triton X-100 for 30 min at 37 ℃ and then blocked with 10% goat serum in PBS for 30 min at room temperature. Thereafter, the primary antibody p-IKKβ

(1:200, Cell Signaling Technology, USA) or MOMA2 (macrophage marker, 1:200, Santa Cruz, Dallas, USA) was subsequently applied to incubate overnight at 4 ℃. PBS without primary antibody was used as negative control. Then, the sections were stained with fluorescence-labelled secondary antibody for 1 h at room temperature and counter-stained with DAPI for 5 min. Finally, the sections were observed under a fluorescence microscope (Olympus Microscope IX3, Japan) and the fluorescence intensity was evaluated using Image J software.

2.13. Statistical analysis

Statistical data are presented as mean ± standard deviation (SD). SPSS software (Version 18.0, https://www.ibm.com/cn-zh/analytics/spss-statistics-software) was used to analyze the data while GraphPad Prism software (version 7.0, https://www.graphpad.com/) was used to generate graphs. One-way ANOVA with Newman-Keuls multiple comparisons test was applied to calculate normal distribution and homogeneous variance, while Dunnett' T3 test was used to calculate non-normal distribution. $P < 0.05$ was considered statistically significant.

3. Results

3.1. SDSS reduced the area of aortic plaque in ApoE$^{-/-}$ mice

As shown in Fig. 1B and Fig. 1C, the aorta of mice in control group appeared smooth and flat without any noticeable plaque formation. In contrast, the model group exhibited evident plaque formation, primarily located at the aortic arch and brachiocephalic trunk, with some flaky plaques observed in the thoracic and abdominal aorta. The plaque distribution in the SDSS and Atorvastatin groups resembled that of the

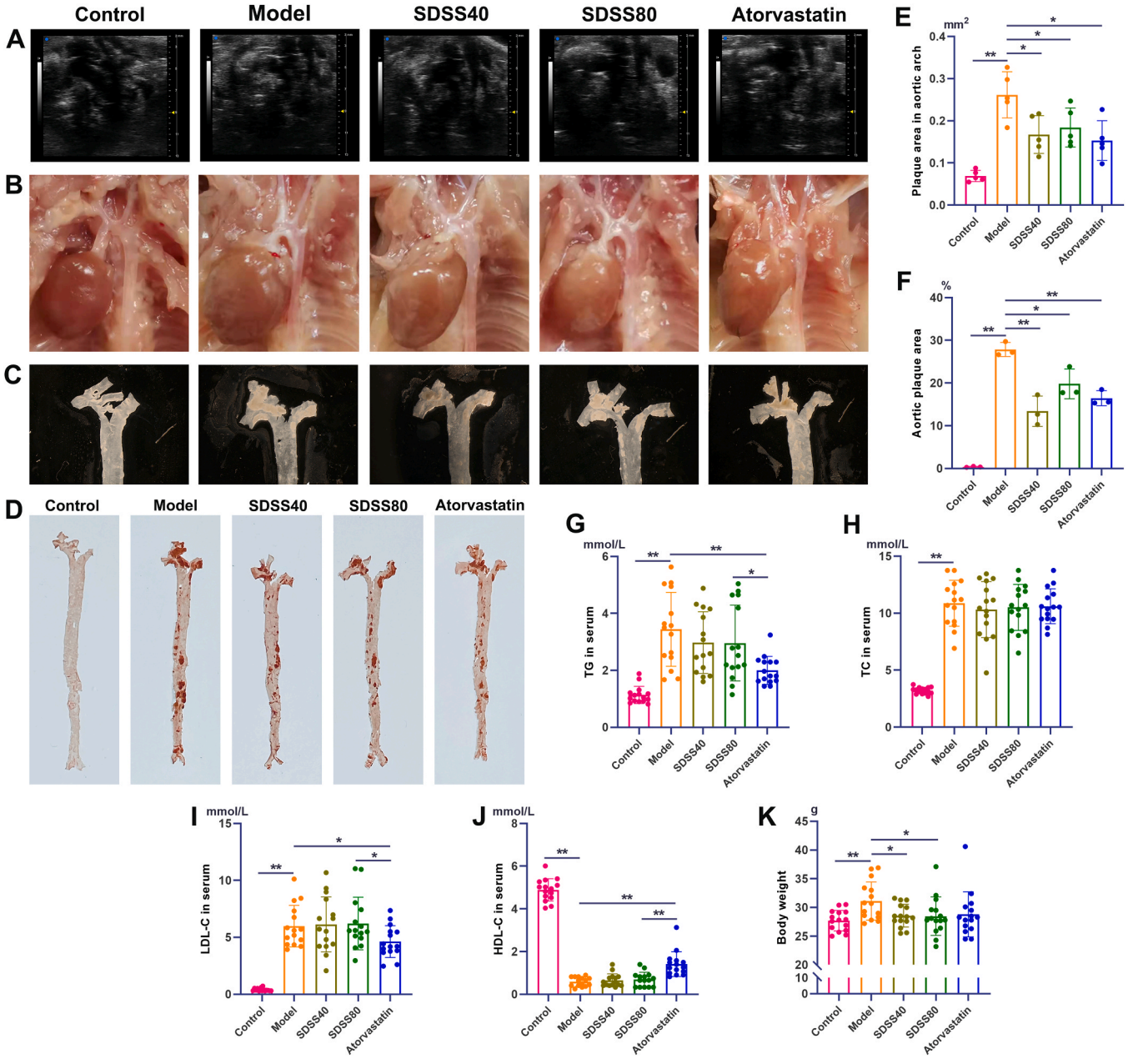

Fig. 1. SDSS reduced the area of aortic plaque in ApoE$^{-/-}$ mice. (A) Representative images of aortic arch ultrasound, (B) Gross appearance of the aorta, (C) Aortic observation of the aorta under the stereoscope, (D) Oil Red O staining of entire aortas, (E) Plaque area in the aortic arch, (F) Aortic plaque area, (G) TG, (H) TC, (I) LDL-C, (J) HDL-C , (K) Body weight in Control, Model, SDSS40, SDSS80 and Atorvastatin group, Data are presented as the mean ± SD. *$P < 0.05$, **$P < 0.01$.

model group, but the plaque area was reduced. Meanwhile, the area of plaque in the aortic arch and aortic root of ApoE$^{-/-}$ mice significantly increased in the model group compared to the control group ($P < 0.01$). However, this increase was attenuated in the SDSS and Atorvastatin groups compared to the model group ($P < 0.05$, $P < 0.01$, Fig. 1A, D-F).

After 24 weeks of high-fat feeding, the body weight of ApoE$^{-/-}$ mice in the model group significantly increased compared to the control group ($P < 0.01$), and SDSS administration reduced the body weight in the model group ($P < 0.05$, Fig. 1K). Moreover, the serum levels of TG, TC, and LDL-C were significantly increased in the model group ($P < 0.01$), while the serum level of HDL-C level was significantly decreased compared to the control group ($P < 0.01$), all of which did not change significantly with SDSS administration. However, atorvastatin administration reduced the serum levels of TG and LDL-C but increased the serum HDL-C level compared to the model group ($P < 0.05$, $P < 0.01$, Fig. 1G-J).

3.2. SDSS reduced the formation of aortic root plaque and stabilized vulnerable plaque in ApoE$^{-/-}$ mice

The fibrous cap thickness, lipid core size, plaque area, and lumen stenosis degree of the aortic root in the model group were significantly increased ($P < 0.01$), whereas the media thickness was significantly decreased compared to the control group ($P < 0.01$). SDSS and atorvastatin administration reduced the lipid core size, plaque area, and luminal stenosis in ApoE$^{-/-}$ mice ($P < 0.05$, $P < 0.01$) and increased the fibrous cap thickness ($P < 0.05$, $P < 0.01$, Fig. 2A, F-J). Meanwhile, the plaque lipid content in the aortic root in the model group was

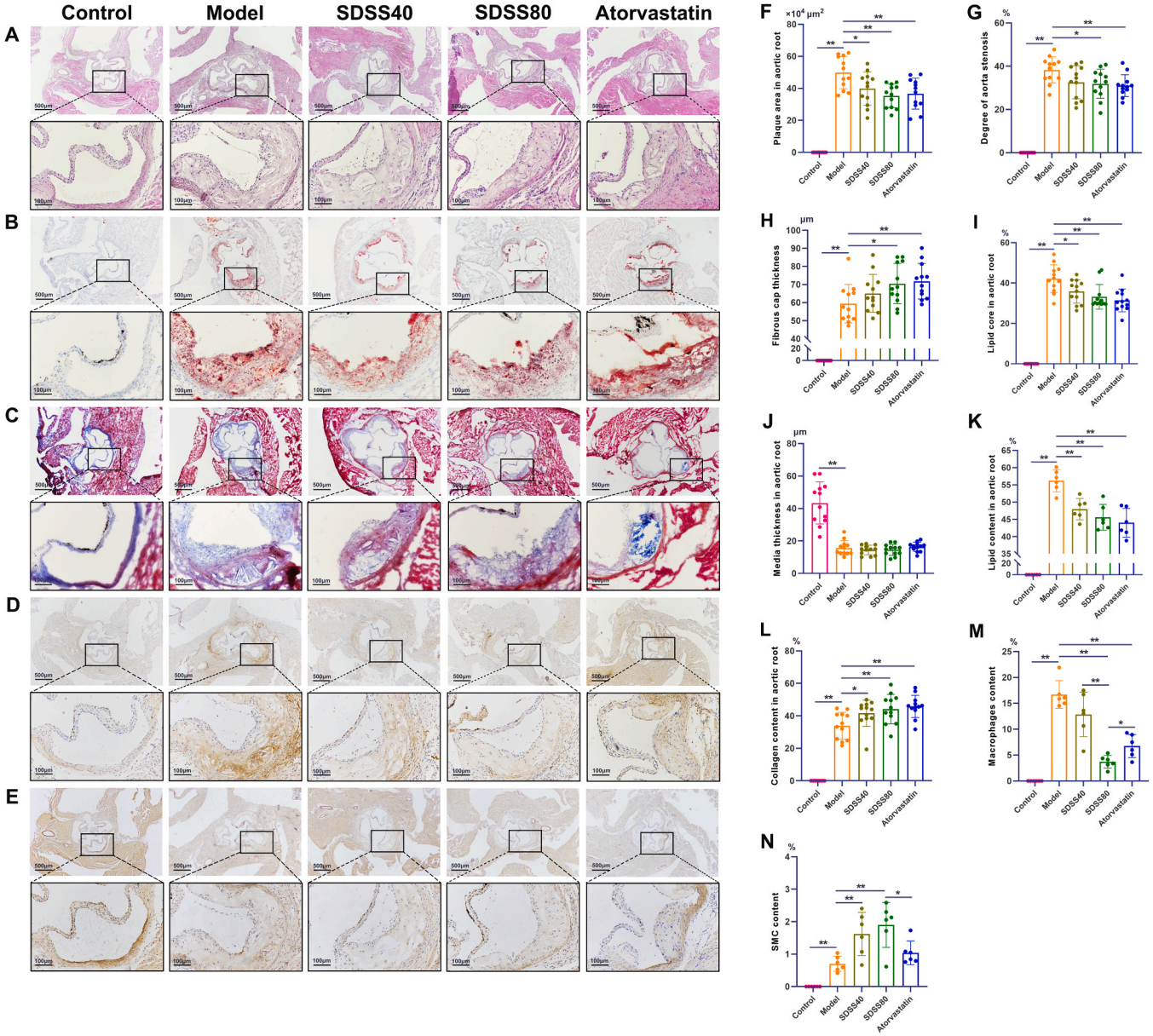

Fig. 2. SDSS reduced the formation of aortic root plaque and stabilized vulnerable plaque in ApoE$^{-/-}$ mice. (A) HE staining, (B) Oil Red O staining, (C) Masson staining (the blue-stained areas are collagen fibers, and the red-stained areas are muscle fibers), (D) MOMA2 immunohistochemical staining, and (E) α-SMA immunohistochemical staining of aortic roots (40 ×, scale bar: 500 μm; 200 ×, scale bar: 100 μm), (F) Plaque area in the aortic root, (G) Degree of aortic stenosis, (H) Fibrous cap thickness, (I) Lipid core in the aortic root, (J) Media thickness in the aortic root, (K) Lipid content in the aortic root (the percentage of the red stained area in the plaque to the plaque area), (L) Collagen content in the aortic root (the percentage of the blue stained area in the plaque to the plaque area), (M) Macrophage content (the percentage of the brown stained area in the plaque to the plaque area), (N) SMC content (the percentage of the brown stained area in the plaque to the plaque area) in Control, Model, SDSS40, SDSS80 and Atorvastatin group, Data are presented as the mean ± SD. *$P < 0.05$, **$P < 0.01$.

significantly increased compared to the control group ($P < 0.01$), SDSS and atorvastatin administration significantly reduced the lipid content respectively ($P < 0.01$, Fig. 2B, K). In addition, the collagen content of plaque at the aortic root in the model group significantly increased compared to the control group ($P < 0.01$), SDSS and atorvastatin administrations increased the collagen content respectively ($P < 0.05$, $P < 0.01$, Fig. 2C, L). Moreover, the number of macrophages within aortic root plaques in model group increased significantly compared to the control group ($P < 0.01$), SDSS80 and atorvastatin administration significantly reduced the number of macrophages ($P < 0.01$), and SDSS80 is of stronger effect than atorvastatin (Fig. 2D, M). Finally, the number of smooth muscle cells (SMC) within plaque in aortic root in model group was significantly increased compared to the control group ($P < 0.01$), and SDSS administration significantly increased the number of SMC ($P < 0.01$, Fig. 2E, N).

3.3. IKKβ is the key binding target of SDSS

The Huprot™ human protein microarray was used to screen the binding proteins of SDSS. First, SDSS was first labeled with biotin. A polyethylene glycol (PEG) ligand was added to increase the water solubility of SDSS-Biotin (Fig. 3A, B). Biotin and SDSS-Biotin binding proteins were then detected using the Huprot™ human protein microarray. Binding performance was then tested using Cy3-conjugated streptavidin (Fig. 3C). A total of 616 proteins were identified as positive binding proteins.

Another approach to target prediction, network pharmacology, was also used to narrow the field. The OMIM, DisGeNET, and PharmGKB databases were meticulously searched using the keyword "atherosclerosis". After merging and deduplication, a total of 2138 AS-related targets were obtained. The 616 SDSS-binding proteins were intersected with the 2138 AS-related targets, so a total of 78 cross-targets were obtained. Then, these 78 targets were imported into the STRING database, and the species was restricted to *Homo sapiens*. The minimum interaction score was set to 0.4 (medium confidence). Finally, 68 targets were screen out. The PPI network was visualized using Cytoscape 3.7.1 software, and the topological properties of the PPI network were analyzed using the Network Analyzer function, and finally 35 core targets were obtained (Table S2). GO enrichment was analyzed from three aspects: biological process (BP), molecular function (MF) and cellular component (CC) using these 35 core targets (Fig. 3F). At the same time, KEGG enrichment analysis was performed using these 35 core targets, and finally a total of 107 pathways were obtained, among which the top 20 pathways were the important pathways (Fig. 3E). It indicated that the important pathways for SDSS to treat AS included Chemokine, T cell receptor, Toll-like receptor, TNF signaling pathways, etc. (Fig. 3E). By analyzing the important pathways and core targets enriched in these pathways, the key effect of SDSS in treating AS was revealed to be inflammation with the key pathway NF-κB signaling pathway. What's more, PI3K, Akt, IKBKB, and NFKB1 in the pathway were regulatory targets (Fig. 3G). Finally, IKBKB (IKKβ) and NFKB1 were identified as key targets since PI3K and Akt targets cannot be directly associated with inflammation.

Molecular docking results revealed that SDSS located at the hydrophobic pocket of IKKβ and NFKB1 proteins. Specifically, the methoxy group of the benzene ring structure interacts with the hydrophobic amino acids Cys99, Asp103, and Lys10 in the hydrophobic pocket of IKKβ proteins, and with amino acid residues Thr143 and Lys144 in the hydrophobic pocket of NFKB1 proteins. They form hydrogen bonds with binding free energies of − 5.16 kcal/mol and − 2.59 kcal/mol, respectively (Fig. 3H).

Comparing the binding free energy and hydrogen bond interaction, SDSS exhibited strong binding activity to IKKβ, suggesting that IKKβ may be the key target of SDSS for treating AS. To confirm the direct binding ability of SDSS to IKKβ, the results of IKKβ and NFKB1 in Huprot™ human protein microarray were further analyzed. As shown in Fig. 3C and Fig. 3D, the average SNR for SDSS-Biotin and Biotin with IKKβ were 107.745 and 4.8125, and the average SNR of SDSS-Biotin and Biotin with NFKB1 were 17.881 and 6.821. The higher the SNR, the better the binding affinity. The above results indicat that SDSS can bind directly to IKKβ with high affinity, but the affinity to NFKB1 is not high, suggesting that IKKβ is the key binding target of SDSS.

3.4. SDSS inhibits NF-κB pathway through targeting IKKβ in vivo

In order to further verify the above results (inflammation is the key effect of SDSS for treating AS, the IKKβ/NF-κB pathway is the key pathway, in which IKKβ is the key target), the following experiments were conducted. As shown in Fig. 4A-K, the serum levels of TNF-α, IL-1β, and IL-6, aortic mRNA transcription levels of TLR4, IKKβ, IKKγ, p65, TNF-α, IL-1β and IL-6, the aorta protein expressions of p-IKKβ, p-IKKβ/IKKβ, p-IκBα, p-IκBα/IκBα, p-p65, p-p65/p65, TNF-α and IL-1β in the model group were increased compared to the control group ($P < 0.05$, $P < 0.01$). Moreover, SDSS administration reduced the levels of TNF-α and IL-1β, down-regulated the mRNA transcription levels of IKKβ, IKKγ, p65, TNF-α, IL-1β and IL-6, decreased the protein expression levels of p-IKKβ, p-IKKβ/IKKβ, p-IκBα, p-IκBα/IκBα, p-p65, p-p65/p65, TLR4, TNF-α and IL-1β ($P < 0.05$, $P < 0.01$).

Meanwhile, as shown in Fig. 4L-O, the fluorescence intensity of p-IKKβ and MOMA2 was significantly increased in the aortic root plaques of the model group compared to the control group, SDSS administration decreased the fluorescence intensity of p-IKKβ and MOMA2 ($P < 0.05$, $P < 0.01$). Furthermore, fluorescence colocalization curve and scatterplot analysis suggested that p-IKKβ could be expressed in macrophages, and the expression of p-IKKβ was closely associated with macrophages, as well as SDSS may inhibit the phosphorylation of IKKβ in macrophages.

3.5. SDSS inhibits NF-κB pathway through targeting IKKβ in vitro

As shown in Fig. 5A-D, the cell viability was significantly decreased in the model group, and the LDH content as well as the levels of TNF-α, IL-1β and IL-6 were significantly increased compared to the control group ($P < 0.01$). Moreover, administration of SDSS (12.5, 25, 50, or 100 μM) increased the cell viability, decreased the LDH content and the levels of TNF-α, IL-1β and IL-6 compared to the model group ($P < 0.05$, $P < 0.01$). Among them, 12.5 μM and 50 μM were the optimal effective dose for further experiment.

Furthermore, as shown in Fig. 5E-O, the mRNA transcription levels of TLR4, IKKβ, p65, TNF-α, IL-1β and IL-6, as well as the protein expression levels of p-IKKβ, p-IKKβ/IKKβ, p-IκBα, p-IκBα/IκBα, p-p65, p-p65/p65, TNF-α, and IL-1β were increased in the macrophages of the model group compared to the control group ($P < 0.05$, $P < 0.01$). In addition, SDSS administration reduced the mRNA transcriptions of IKKβ, TLR4, p65, TNF-α, IL-1β and IL-6, and down-regulated the protein expressions of p-IKKβ, p-IKKβ/IKKβ, p-IκBα, p-IκBα/IκBα, p-p65, p-p65/p65, TNF-α and IL-1β ($P < 0.05$, $P < 0.01$).

3.6. IMD-0354 enhanced the effect of SDSS

As shown in Fig. 6A-D, administration of SDSS50, IMD and SDSS50-IMD both increased the cell viability and decreased the LDH content as well as TNF-α, IL-1β and IL-6 levels ($P < 0.05$, $P < 0.01$). Compared to the SDSS50 group, the levels of IL-6 were decreased in SDSS50-IMD group ($P < 0.05$, $P < 0.01$). Meanwhile, as shown in Fig. 6E-L, SDSS50, IMD, and SDSS50-IMD administration down-regulated the mRNA transcriptions of IKKβ, TNF-α and IL-6, reduced the protein expressions of p-IKKβ, p-IKKβ/IKKβ, p-IκBα, p-IκBα/IκBα, p-p65, p-p65/p65, TNF-α and IL-1β ($P < 0.05$, $P < 0.01$). In addition, SDSS50 and SDSS50-IMD administration decreased the transcriptions of TLR4 and IL-1β, while IMD and SDSS50-IMD administration decreased the transcription of p65 ($P < 0.05$). Compared to the SDSS50 group, the

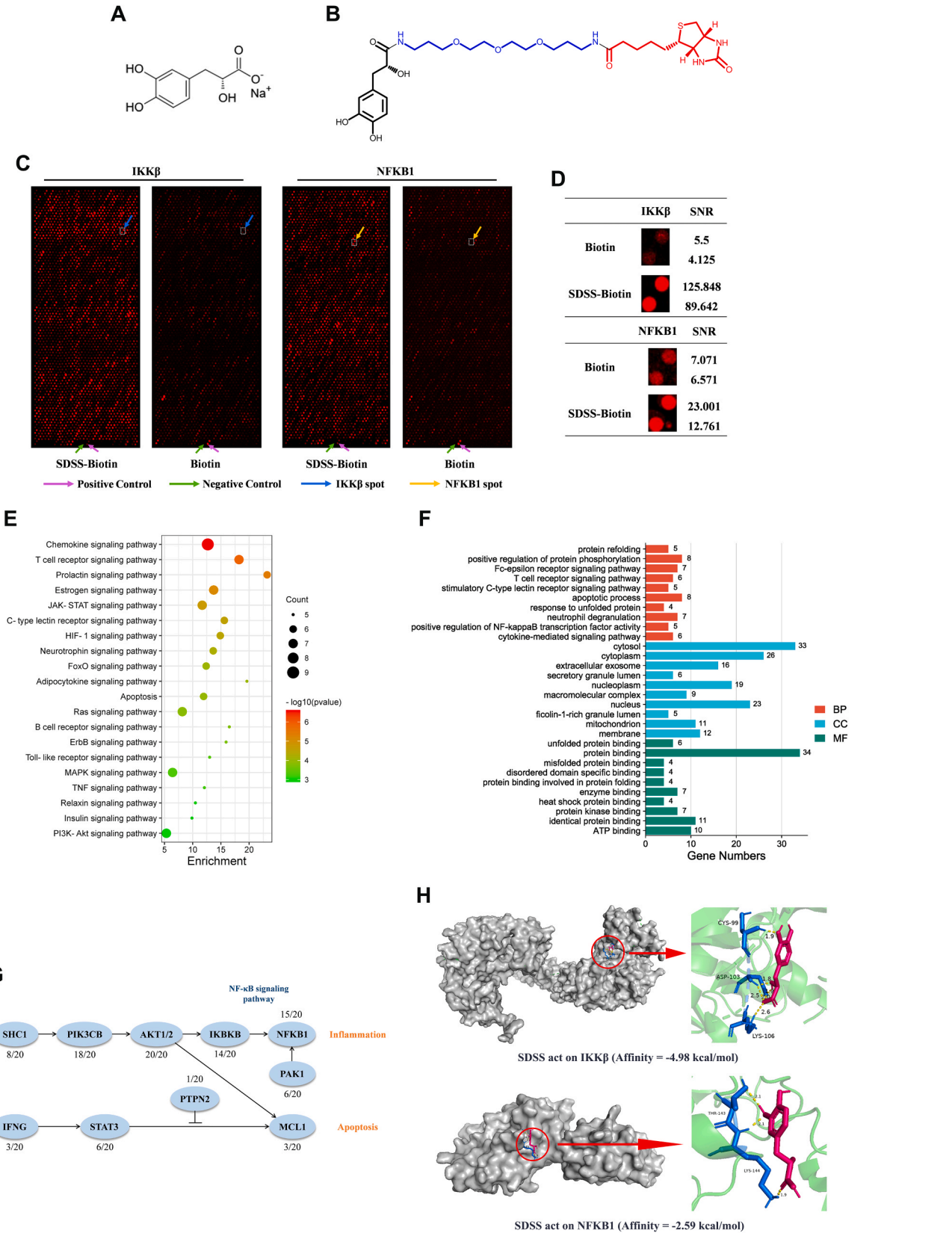

Fig. 3. IKKβ is the key binding target of SDSS. (A) The chemical structure of SDSS and (B) biotin-labeled SDSS (Bio-SDSS). The blue color represents PEG ligand and the red color represents biotin. (C) Representative image of protein array, including positive control spots (Bio-SDSS) and negative control spots (Biotin), as well as the enlarged image of Bio-SDSS binding to IKKβ and NFKB1. The SNR is shown in (D). (E) KEGG pathway analysis and (F) GO enrichment analysis of core targets. (G) Key effects analysis. (H) Molecular docking interaction of SDSS with the binding site of the IKKβ and NFKB1 proteins.

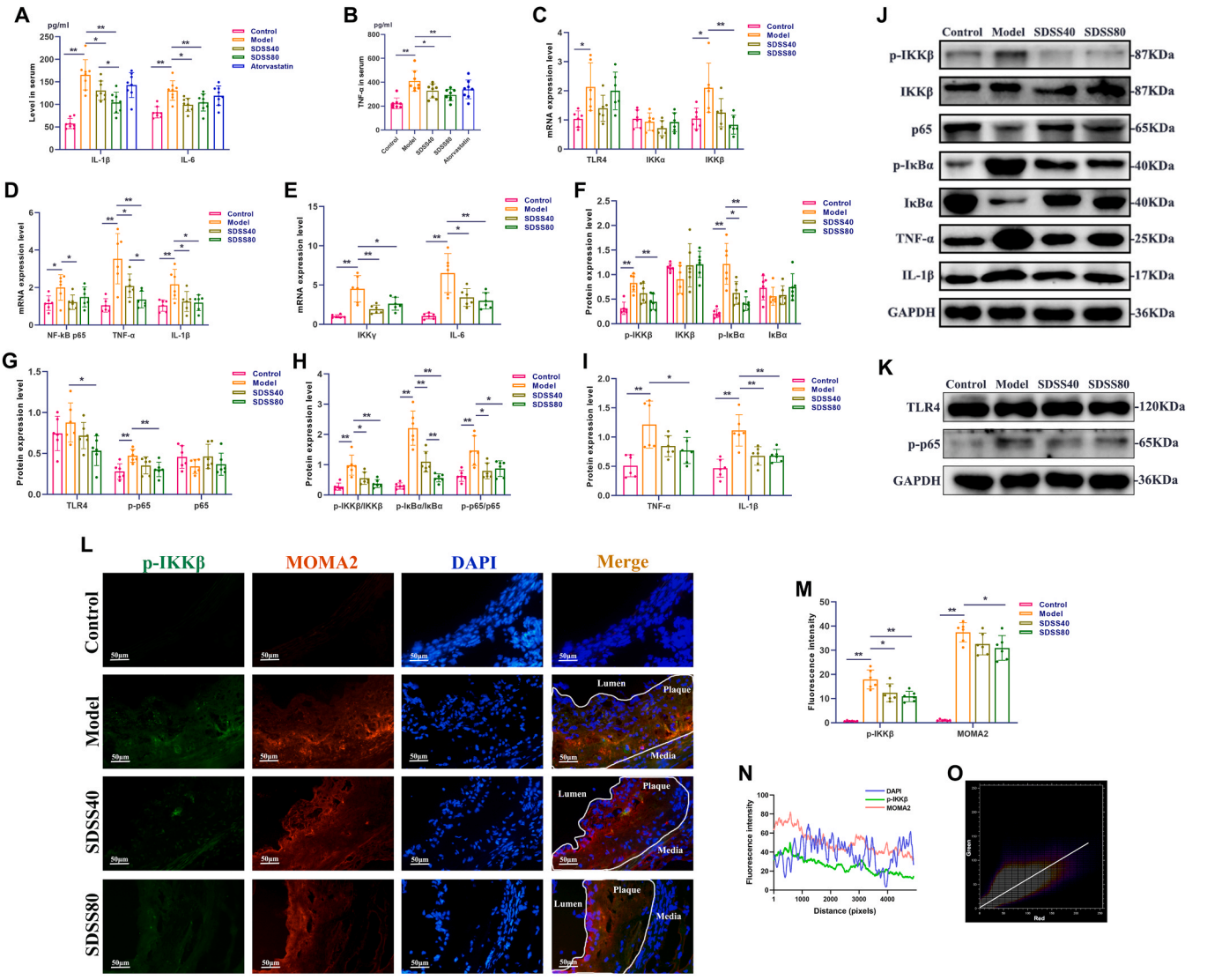

Fig. 4. SDSS inhibits NF-κB pathway through targeting IKKβ in vivo. (A) IL-1β, IL-6, and (B) TNF-α levels in serum. (C) TLR4, IKKα, IKKβ, (D) NF-κB (p65), TNF-α, IL-1β, and (E) IKKγ, IL-6 mRNA transcription levels in aorta. (F) p-IKKβ, IKKβ, p-IκBα, IκBα, (G) TLR4, p-p65, p65, (H) p-IKKβ/IKKβ, p-IκBα/IκBα, p-p65/p65, and (I) TNF-α, IL-1β protein expression levels in aorta. (J) p-IKKβ, IKKβ, p65, p-IκBα, IκBα, TNF-α, IL-1β and (K) TLR4, p-p65 protein expression levels in aorta. (L) Double fluorescence staining of p-IKKβ and MOMA2 in the aortic root plaque (400 ×, scale bar: 50 μm), the area enclosed by the white circle represents the plaque area, and white arrows indicate the expression of p-IKKβ in macrophages. (M) Fluorescence intensity of p-IKKβ and MOMA2. (N) Fluorescence colocalization curve. (O) Fluorescence colocalization scatterplot. GAPDH served as an internal control, and data are presented as the mean ± SD. *$P < 0.05$, **$P < 0.01$.

transcriptions of TNF-α and IL-6, the protein expression of IκBα decreased in SDSS50-IMD group ($P < 0.05$, $P < 0.01$).

4. Discussion

In this study, SDSS administration inhibits AS plaque formation and improves the degree of aortic stenosis in vivo (Fig. 1). Moreover, subintimal lipid deposition caused by hyperlipidemia is the material basis of AS, and the ApoE$^{-/-}$ mice used in this study exhibited hyperlipidemia, but SDSS administration has no effect on the blood lipid level, indicating that the mechanism of SDSS in stabilizing vulnerable plaque is independent of lipid regulation. Different from the above results, other researches indicated that Danshensu can significantly correct hyperlipidemia in AS rats, including reduced serum TC, TG, and LDL-C levels, as well as gradually improved the descending trend of serum HDL-C levels [18]. Meanwhile, SDSS administration reduced the area, lipid content and macrophage infiltration of the aortic root plaque, while increased collagen content and SMC recruitment, indicating that SDSS reduced the aortic root plaque formation and stabilize vulnerable plaque (Fig. 2). At present, there are almost no studies on the treatment of AS with SDSS, Danlou tablets (containing Danshensu as one of the main components) attenuated the plaque size; reduced lipid content in the brachiocephalic trunk, aortic arch and aortic root in ApoE$^{-/-}$ mice fed a high-fat diet for 20 weeks [17].

Furthermore, it has been established that the key effect of SDSS in treating AS is inflammation, the key pathway is the IKKβ/NF-κB pathway, and the key binding target is IKKβ (Fig. 3). NF-κB is an important transcription factor involved in the regulation of cell proliferation, survival and inflammation [22]. There are many stimuli that can activate NF-κB, including pro-inflammatory factors, infectious agents, reactive oxygen species, free fatty acids, etc. [23]. Stimulants such as pro-inflammatory factors and growth factors can activate membrane-bound receptors such as tumor necrosis factor receptor (TNFR), interleukin-1 receptor (IL-1R) and Toll-like receptor (TLR), which in turn activate the IκB kinase (IKK) complex [24]. IKK is usually composed of IKKα, IKKβ and IKKγ [25]. IKKβ can phosphorylate IκB to

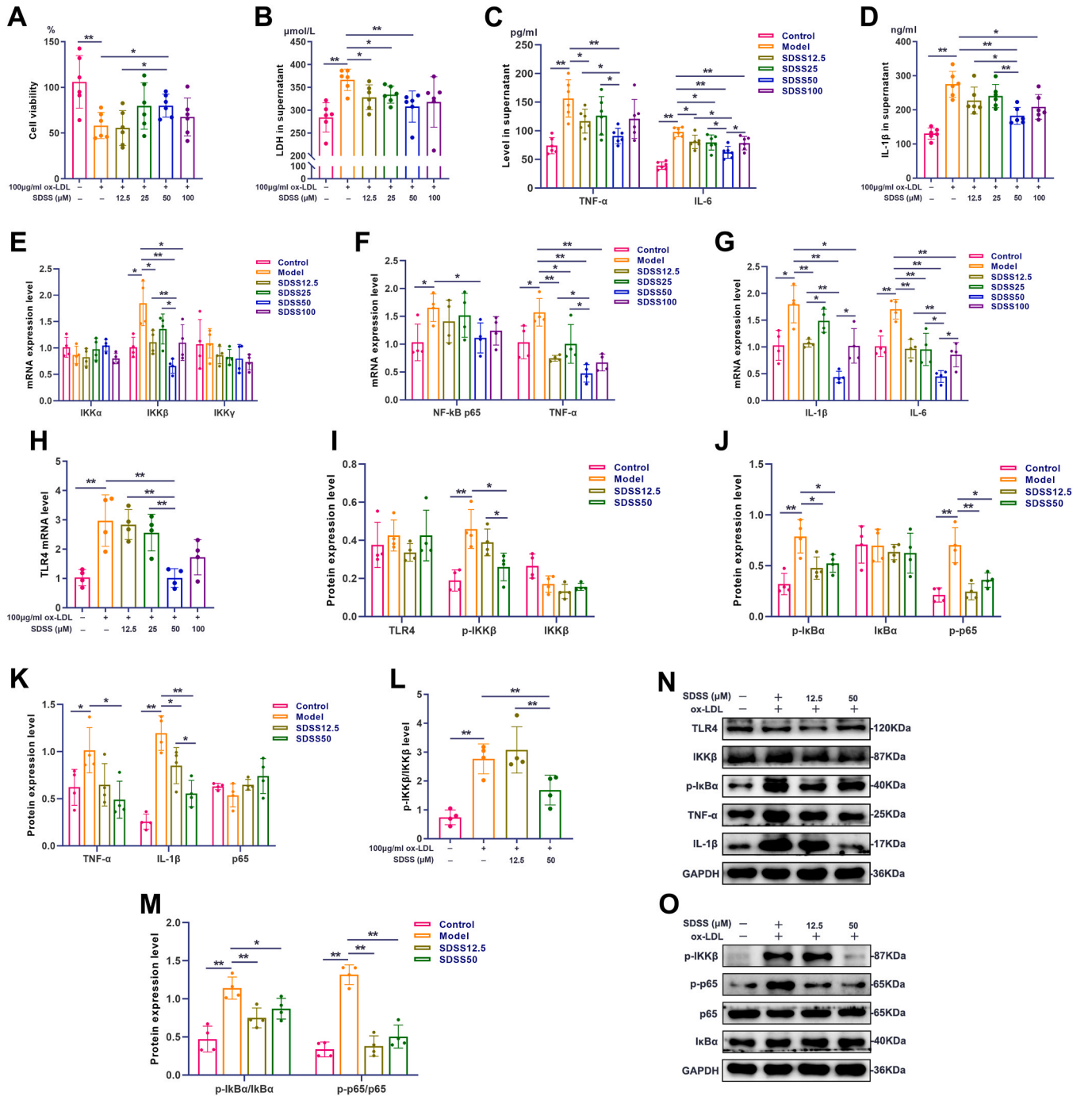

Fig. 5. SDSS inhibits NF-κB pathway through targeting IKKβ in vitro. (A) Cellular viability for J774A.1 cells were treated with SDSS after ox-LDL. (B) LDH, (C) TNF-α, IL-6, (D) IL-1β levels in cell culture supernatants. (E) IKKα, IKKβ, IKKγ, (F) NF-κB (p65), TNF-α, (G) IL-1β, IL-6, and (H) TLR4 mRNA transcription levels in J774A.1 cells. (I) TLR4, p-IKKβ, IKKβ, (J) p-IκBα, IκBα, p-p65, (K) TNF-α, IL-1β, p65, (L) p-IKKβ/IKKβ, and (M) p-IκBα/IκBα, p-p65/p65 protein expression levels in J774A.1 cells. (N) TLR4, IKKβ, p-IκBα, TNF-α, IL-1β and (O) p-IKKβ, p-p65, p65, IκBα protein expression levels in J774A.1 cells. GAPDH served as an internal control, and data were presented as the mean ± SD. $^{*}P < 0.05$, $^{**}P < 0.01$.

promote the release and nuclear translocation of active NF-κB [13]. Thus, IKKβ is a key subunit for the activation of the canonical NF-κB signaling pathway. Several studies demonstrated that the IKKβ/NF-κB pathway plays role in macrophages to promote AS formation. For example, the overexpression of transdominant and non-degradable form of IκBα inhibits NF-κB signaling in macrophages, thereby reducing macrophage foam cell formation in vitro [26]. Meanwhile, myeloid-specific IKKβ deficiency reduced high-fat-induced atherosclerotic plaque formation in LDLR$^{-/-}$ mice by reducing macrophage adhesion, migration, lipid uptake, and other inflammatory responses [14]. Taken together, these studies suggest a complex role for IKKβ/NF-κB pathway in macrophage inflammation and AS development.

Moreover, SDSS administration reduced the levels of TNF-α, IL-1β and IL-6, down-regulated the transcriptions and protein expressions of IKKβ/NF-κB pathway related targets (TLR4, p-IKKβ, IKKβ, IKKγ, IκBα, p-IκBα, p-p65, p65, TNF-α, IL-1β, IL-6) in vivo and in vitro, inhibited the phosphorylation of IKKβ in macrophages in vivo, indicating that SDSS suppressed the inflammation and inhibited the IKKβ/NF-κB pathway, as well as IKKβ is the key target (Figs. 4, 5). Similar to the above results, a study showed that Danshensu treatment reduced IL-1β, IL-6, TNF-α

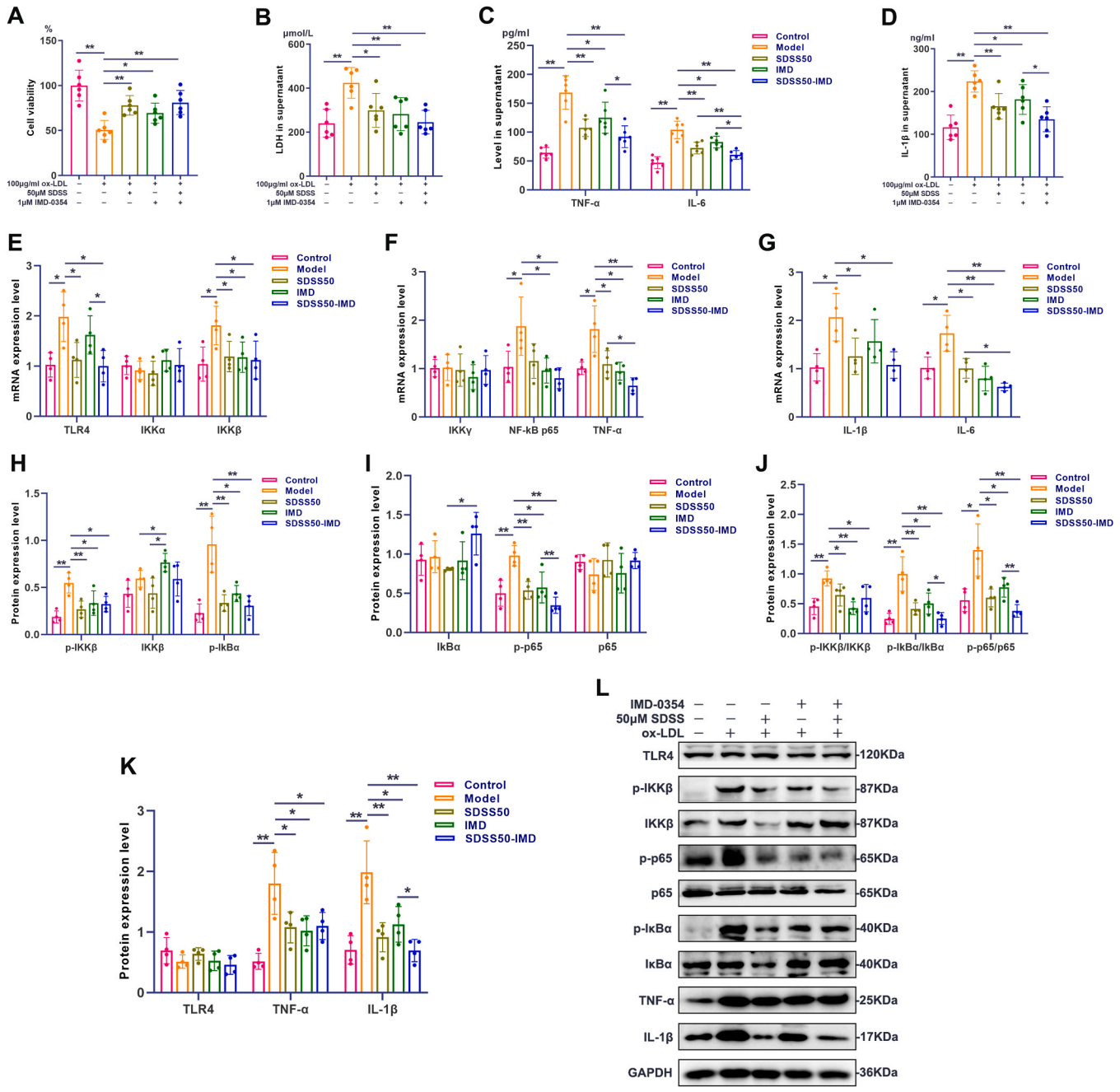

Fig. 6. IMD-0354 enhanced the effect of SDSS. (A) Cellular viability for J774A.1 cells were treated with SDSS and IMD-0354 after ox-LDL. (B) LDH, (C) TNF-α, IL-6, (D) IL-1β levels in cell culture supernatants. (E) TLR4, IKKα, IKKβ, (F) IKKγ, NF-κB (p65), TNF-α, and (G) IL-1β, IL-6 transcription levels in J774A.1 cells. (H) p-IKKβ, IKKβ, p-IκBα, (I) IκBα, p-p65, p65, (J) p-IKKβ/IKKβ, p-IκBα/IκBα, p-p65/p65, and (K) TLR4, TNF-α, IL-1β protein expression levels in J774A.1 cells. (L) TLR4, p-IKKβ, IKKβ, p-p65, p65, p-IκBα, IκBα, TNF-α, and IL-1β protein expression levels in J774A.1 cells. GAPDH served as an internal control, and data were presented as the mean ± SD. $^{*}P < 0.05$, $^{**}P < 0.01$.

levels in the serum and TLR4, p-IκBα, and p-NF-κB (p65) expression levels in AS rats and ox-LDL-induced HUVECs through inhibiting the TLR4/NF-κB signaling pathway [18]. Furthermore, SDSS also has anti-inflammatory effects in other diseases, and is closely related to the IKKβ/NF-κB signaling pathway. For example, Danshensu administration down-regulated the phosphorylation level of NF-κB p65, IKKβ and IκBα in kidney tissues and HK-2 cells [27], inhibited the expression of IL-6 and IL-12, suppressed the phosphorylation of p65 in TLR2-triggered macrophages via NF-κB activation [28], reduced IL-1β-induced phosphorylation of p-IκBα and p-p65 by regulating NF-κB signaling pathway in a dose-dependent manner in chondrocytes [29].

Finally, the addition of IKKβ-specific inhibitor IMD-0354 inhibited the IKKβ/NF-κB pathway by targeting IKKβ to suppress the inflammatory responses, and enhance the effect of SDSS on ox-LDL-induced macrophages in this study (Fig. 6). Similarly, research showed that IMD-0354 (0.25, 0.5, 1 μM) administration decreased the phosphorylation levels of IKKβ, IκBα, and p65 in osteoclasts in a dose-dependent manner [30]. Molecular docking results indicated that SDSS binds to IKKβ that exhibits competitive ATP-binding activity to inhibit IKKβ phosphorylation. However, a recent ATP-based kinase assay showed that IMD-0354 has no activity against IKKβ or IKKα [31], suggesting that IMD-0354 does not competitively inhibit SDSS in inhibiting non-ATP binding. Therefore, there will be a synergistic effect when SDSS intervenes with IMD-0354.

However, future research should address several issues. Firstly, there is a lack of studies examining the in-depth mechanism of anti-inflammation and the treatment of AS by SDSS. Most existing studies mainly focus on reducing the levels of inflammatory cytokines, with limited research on specific targets and pathways. Secondly, it is crucial to conduct clinical trials to further investigate the therapeutic effects of SDSS, as current research primarily relies on cell and animal studies. This study is the first to confirm that SDSS can stabilize vulnerable plaques by targeting and inhibiting IKKβ, suppressing the IKKβ/NF-κB pathway, and mitigating inflammatory responses. However, more research is needed to fully understand these mechanisms.

Funding Source

All sources of funding should be acknowledged, and you should declare any extra funding you have received for academic research of this work. If there are none state 'there are none'.

CRediT authorship contribution statement

Miao Zeng: Investigation, Writing – original draft. **Xiaolu Zhang**: Investigation, Writing – original draft. **Nuan Lv**: Writing – review & editing, Supervision. **Luming Wang**: Writing – review & editing, Supervision. **Yanrong Suo**: Conceptualization, Project administration, Funding acquisition. **Jiali Gan:** Writing – review & editing, Supervision. **Lin Yang**: Writing – review & editing, Supervision. **Bin Yu**: Writing – review & editing, Supervision. **Xijuan Jiang**: Conceptualization, Project administration, Funding acquisition. **Wenyun Zeng**: Conceptualization, Project administration, Funding acquisition.

Declaration of Competing Interest

Please declare any financial or personal interests that might be potentially viewed to influence the work presented. Interests could include consultancies, honoraria, patent ownership or other. If there are none state 'there are none'.

Acknowledgments

This study was supported by National Natural Science Foundation of China (No. 82074211, 82160828), Natural Science Foundation of JiangXi Province (No. 20224BAB206116, 20171ACB21075), Tianjin Graduate Research Innovation Project (No. 2022BKY188), TUTCM Graduate Research Innovation Project (No. YJSKC-20221006), and 2021 Annual Graduate Students Innovation Fund (School of Integrative Medicine, Tianjin University of Traditional Chinese Medicine, Tianjin, China; No. ZXYCXLX202102).

Appendix A. Supporting information

Supplementary data associated with this article can be found in the online version at doi:10.1016/j.biopha.2023.115153.

References

[1] M. Rafieian-Kopaei, et al., Atherosclerosis: process, indicators, risk factors and new hopes, Int. J. Prev. Med. 5 (8) (2014) 927–946.
[2] O. Soehnlein, Multiple roles for neutrophils in atherosclerosis, Circ. Res. 110 (6) (2012) 875–888, https://doi.org/10.1161/CIRCRESAHA.111.257535.
[3] Y. Asada, et al., Pathophysiology of atherothrombosis: Mechanisms of thrombus formation on disrupted atherosclerotic plaques, Pathol. Int 70 (6) (2020) 309–322, https://doi.org/10.1111/pin.12921.
[4] P. Libby, et al., Atherosclerosis, Nat. Rev. Dis. Prim. 5 (1) (2019) 56, https://doi.org/10.1038/s41572-019-0106-z.
[5] F. Liu, et al., Bionic microbubble neutrophil composite for inflammation-responsive atherosclerotic vulnerable plaque pluripotent intervention, Res. (Wash. D.C.) (2022) 9830627, https://doi.org/10.34133/2022/9830627.
[6] L.C. Winkel, et al., Folate receptor-targeted single-photon emission computed tomography/computed tomography to detect activated macrophages in atherosclerosis: can it distinguish vulnerable from stable atherosclerotic plaques? Mol. Imaging (2014) 13, https://doi.org/10.2310/7290.2013.00061.
[7] J. Zhou, et al., Platelet membrane biomimetic nanoparticles combined with UTMD to improve the stability of atherosclerotic plaques, Front Chem. 10 (2022), 868063, https://doi.org/10.3389/fchem.2022.868063.
[8] A. Seneviratne, et al., Biomechanical factors and macrophages in plaque stability, Cardiovasc Res. 99 (2) (2013) 284–293, https://doi.org/10.1093/cvr/cvt097.
[9] J. Tang, et al., Inhibiting macrophage proliferation suppresses atherosclerotic plaque inflammation, Sci. Adv. 1 (3) (2015), https://doi.org/10.1126/sciadv.1400223.
[10] M.H. Gwon, et al., Phenethyl isothiocyanate protects against high fat/cholesterol diet-induced obesity and atherosclerosis in C57BL/6 mice, Nutrients 12 (12) (2020), https://doi.org/10.3390/nu12123657.
[11] M.P. de Winther, et al., Nuclear factor kappaB signaling in atherogenesis, Arterioscler. Thromb. Vasc. Biol. 25 (5) (2005) 904–914, https://doi.org/10.1161/01.ATV.0000160340.72641.87.
[12] J.H. An, et al., LncRNA SNHG16 promoted proliferation and inflammatory response of macrophages through miR-17-5p/NF-kappaB signaling pathway in patients with atherosclerosis, Eur. Rev. Med. Pharm. Sci. 23 (19) (2019) 8665–8677, https://doi.org/10.26355/eurrev_201910_19184.
[13] M. Yin, et al., Reduced SULT2B1b expression alleviates ox-LDL-induced inflammation by upregulating miR-148–3 P via inhibiting the IKKbeta/NF-kappaB pathway in macrophages, Aging (Albany NY) 13 (3) (2021) 3428–3442, https://doi.org/10.18632/aging.202273.
[14] S.H. Park, et al., Myeloid-specific IkappaB kinase beta deficiency decreases atherosclerosis in low-density lipoprotein receptor-deficient mice, Arterioscler. Thromb. Vasc. Biol. 32 (12) (2012) 2869–2876, https://doi.org/10.1161/ATVBAHA.112.254573.
[15] J. Zhang, et al., Therapeutic potentials and mechanisms of the Chinese traditional medicine Danshensu, Eur. J. Pharm. 864 (2019), 172710, https://doi.org/10.1016/j.ejphar.2019.172710.
[16] J. Li, et al., Anti-osteogenic effect of danshensu in ankylosing spondylitis: an in vitro study based on integrated network pharmacology, Front Pharm. 12 (2021), 772190, https://doi.org/10.3389/fphar.2021.772190.
[17] D. Hao, et al., Ethanol extracts of Danlou tablet attenuate atherosclerosis via inhibiting inflammation and promoting lipid effluent, Pharm. Res. 146 (2019), 104306, https://doi.org/10.1016/j.phrs.2019.104306.
[18] Q. Song, et al., Potential mechanisms underlying the protective effects of salvianic acid A against atherosclerosis in vivo and vitro, Biomed. Pharm. 109 (2019) 945–956, https://doi.org/10.1016/j.biopha.2018.10.147.
[19] X.W. Wenjun Wang, H.L. Zhi Yao, The influence of emodin and danshensu on monocyte secretion of inflammatory cytokines, Chin. J. Immunol. 11 (1995) 370–372.
[20] J. Jiang, et al., High-throughput determination of sodium danshensu in beagle dogs by the LCMS/MS method, employing liquid-liquid extraction based on 96-well format plates, Molecules 22 (5) (2017), https://doi.org/10.3390/molecules22050667.
[21] T. Zhao, et al., DNA methylation-regulated QPCT promotes sunitinib resistance by increasing HRAS stability in renal cell carcinoma, Theranostics 9 (21) (2019) 6175–6190, https://doi.org/10.7150/thno.35572.
[22] N.D. Perkins, Integrating cell-signalling pathways with NF-kappaB and IKK function, Nat. Rev. Mol. Cell Biol. 8 (1) (2007) 49–62, https://doi.org/10.1038/nrm2083.
[23] M.S. Hayden, S. Ghosh, Shared principles in NF-kappaB signaling, Cell 132 (3) (2008) 344–362, https://doi.org/10.1016/j.cell.2008.01.020.
[24] B. Ma, M.O. Hottiger, Crosstalk between Wnt/beta-Catenin and NF-kappaB signaling pathway during inflammation, Front Immunol. 7 (2016) 378, https://doi.org/10.3389/fimmu.2016.00378.
[25] A. Piotrowska, et al., The structure of NF-kappaB family proteins and their role in apoptosis, Post. Hig. Med. Dosw (Online) 62 (2008) 64–74.
[26] V. Ferreira, et al., Macrophage-specific inhibition of NF-kappaB activation reduces foam-cell formation, Atherosclerosis 192 (2) (2007) 283–290, https://doi.org/10.1016/j.atherosclerosis.2006.07.018.
[27] C. Yu, et al., Danshensu attenuates cisplatin-induced nephrotoxicity through activation of Nrf2 pathway and inhibition of NF-kappaB, Biomed. Pharm. 142 (2021), 111995, https://doi.org/10.1016/j.biopha.2021.111995.
[28] T. Ye, et al., Inhibition of nuclear factor kappa B as a mechanism of Danshensu during Toll-like receptor 2-triggered inflammation in macrophages, Int. Immunopharmacol. 83 (2020), 106419, https://doi.org/10.1016/j.intimp.2020.106419.
[29] Z. Xu, et al., Danshensu inhibits the IL-1beta-induced inflammatory response in chondrocytes and osteoarthritis possibly via suppressing NF-kappaB signaling pathway, Mol. Med. 27 (1) (2021) 80, https://doi.org/10.1186/s10020-021-00329-9.
[30] W. Chen, et al., The emerging role of IMD 0354 on bone homeostasis by suppressing osteoclastogenesis and bone resorption, but without affecting bone formation, Cell Death Dis. 10 (9) (2019) 654, https://doi.org/10.1038/s41419-019-1914-5.
[31] A.C. Pippione, et al., 4-Hydroxy-N-[3,5-bis(trifluoromethyl)phenyl]-1,2,5-thiadiazole-3-carboxamide: a novel inhibitor of the canonical NF-kappaB cascade, Medchemcomm 8 (9) (2017) 1850–1855, https://doi.org/10.1039/c7md00278e.